HAL
open science

Structure and morphological study of nanometer W and W3O thin films

Laurence Maillé, C. Sant, C. Le Paven-Thivet, C. Legrand-Buscema, Pierre Garnier

To cite this version:

Laurence Maillé, C. Sant, C. Le Paven-Thivet, C. Legrand-Buscema, Pierre Garnier. Structure and morphological study of nanometer W and W3O thin films. Thin Solid Films, 2003, 428 (1-2), pp.237 - 241. 10.1016/S0040-6090(02)01277-4 . hal-01845323

HAL Id: hal-01845323

https://hal.science/hal-01845323v1

Submitted on 20 Jul 2018

HAL is a multi-disciplinary open access archive for the deposit and dissemination of scientific research documents, whether they are published or not. The documents may come from teaching and research institutions in France or abroad, or from public or private research centers.

L'archive ouverte pluridisciplinaire **HAL**, est destinée au dépôt et à la diffusion de documents scientifiques de niveau recherche, publiés ou non, émanant des établissements d'enseignement et de recherche français ou étrangers, des laboratoires publics ou privés.

PAPER REFERENCE : J/PI.31

STRUCTURE AND MORPHOLOGICAL STUDY OF NANOMETER W AND W_3O THIN FILMS

L. Maillé*, C. Sant, C. Le Paven-Thivet, C. Legrand-Buscema and P. Garnier

Laboratoire d'étude des Milieux Nanométriques, Université d'Evry Val d'Essonne, Institut des sciences, Rue du Père Jarlan - 91023 Evry Cedex, France

Abstract

In this paper, the structure of nanometer tungsten thin films has been correlated to their surface morphology. Films have been deposited by RF-sputtering at a working pressure of 0.5 Pa and with a power density of 1.18 W/cm^2. Two phases with different morphology has been observed : W_3O with a nanograins structure is present in the first step of the tungsten growth; and, when the

* Corresponding author: Tel. +33-1-69477696; Fax. +33-1-69477696;
E-mail address: laurence.maille@univ-evry.fr

thickness is increased, a pure tungsten Wolfram phase (W) with a lamellar structure appears. We demonstrate that W_3O is related to a pollution of the target surface between two growth runs. We succeed to suppress this phase and to obtain pure tungsten Wolfram nanolayer, in order to realize $[W/WO_3]_n$ multilayer.

Keywords: RF-sputtering; tungsten thin films; W_3O structure; W structure; Atomic Force Microscopy; X-Ray diffraction.

---

1. Introduction

Nanomaterials possess original physical properties. Many searchers study about mechanical [1-4]; optical [5-6], electrical [4;7] or magnetical [4] properties. On the other hand, tungsten is a material well known for its particular characteristics : high hardness, high melting point, low coefficient of friction, resistance against oxidation and corrosion [1;8]. We purpose the study of the mechanical properties of tungsten nanomaterial.

X-Ray diffraction patterns analysis of tungsten layers often show the existence of two phases [9-10]. The pure tungsten Wolfram (W) wished; and a second one that was determined to be a low oxidized tungsten phase, W_3O-A15 also called β-W. This unwished phase exists in the very first step of the tungsten films growth.

Our purpose is to realize multilayer structure W/WO_x and W/WN_x with some nanometers of thickness. In these nanolaminated structures, the individual layer thickness is lower than 50 nm. Then, the unwished W_3O phase will dramatically perturb the mechanical properties of multilayers. The oxidized tungsten phase must be absolutely avoided. The objective of this work is to control pure W Wolfram nanolayer elaboration for monolithic layer and multilayer.

2. Experimental procedure

2.1. Thin films deposition

Tungsten films are deposited at room temperature by R.F-sputtering. The working pressure during deposition is 0,5 Pa. The sputtering target (127 mm of diameter) consist in of pure tungsten element metal. Tungsten films are grown using pure argon plasma. WO_3 films are deposited by a reactive R.F-sputtering with an atmosphere composed of an Ar + O_2 (20%) mixture. The target-substrate distance is kept constant at 70 mm. During deposition, the power density on the tungsten target is 1,18 W/cm^2. <100> silicon wafers are used. A shutter can be placed between the sputter source and the substrate, in order to prevent the layer deposition during the target cleaning process and to allow the multilayer realisation.

Three kinds of samples have been processed :

- Tungsten monolayers without target cleaning and with different thicknesses;
- Tungsten monolayers with a target cleaning before deposition;
- Tungsten monolayers with a target cleaning before deposition and with a target cleaning after a fictitious WO_3 layer. The experimental procedure of this third type of sample is described below.

In order to analyse the structure of the tungsten layers in the multilayer $[W/WO_3]_n$, we have grown a tungsten layer in the same conditions rather than during the multilayer process. We have first cleaned the target during 1 hour. WO_3 layer (50 nm of thickness) is grown by a reactive RF sputtering (Ar + O_2 (20%) mixture); with the shutter closed. The WO_3 growth is then performed on the shutter and not on the wafer. This layer is then called “fictitious” WO_3 layer. At the end of this fictitious layer, the O_2 reactive gas is removed from the chamber. A target cleaning of the target surface is performed before the W Wolfram film deposition. 1, 3 and 5 minutes have been chosen for target cleaning after the remove of the oxygen gas from the growth chamber. The W layer is then deposited. The so obtained layer is a tungsten one, grown in the same condition rather than during $[W/WO_3]_1$ multilayer growth.

2.2. Thin films characterisations

A Bruker D8 Advance X-Ray Diffractometer (XRD) is used to investigate film structure, employing the Cu-Kα radiation and Ni filter. Film surfaces are observed by Atomic Force Microscopy (AFM tapping mode), using a Digital Instruments 3100. X-Ray reflectometry (XRR) (Bruker D8 Advance) and AFM are used to check the surface's roughness. Thicknesses are simulated by a spectrum fit of XRR if it is smaller than 100nm. Otherwise they are observed on cross section by a Scanning Electron Microscopy (SEM), using a Zeiss DSM982 Gemini SEM.

3. Results

3.1. XRD patterns analysis

X-Ray diffraction patterns analysis performed on very thin tungsten layers show the existence of two phases : W Wolfram (W) and a low oxidized tungsten phase W_3O-A15 (β-W). W is thermodynamically stable form under ordinary conditions. It is a body centered cubic structure with a cell of 3,1648 Å and a density of 19,262 (JCPDS file 4-806). W_3O has been reported by A. Katagiri *et al.* to be an intermediate phase before the growth of pure W [11]. It is a cubic structure with a cell of 5,047 Å and a density of 14,662 (JCPDS file 41-1230). The nature of this oxide has been described by several authors [9-15]. XRD patterns analysis show that W_3O peaks are observed in the thin films when thicknesses are smaller than 100 nm.

Figure 1 a, b and c present XRD patterns of tungsten thin films with different thickness : 48 nm; 94 nm and 175 nm respectively. XRD patterns are performed between $2\theta = 30°$ to 130°. In figure 1, only the 34°-46° range is presented since no significant peaks were found elsewhere. When the thickness increases, the intensity of W_3O peaks decreases whereas the intensity of W peaks increases.

3.2. Surface morphology

AFM analysis show a change of the surface morphology of these films when the thickness increases (fig.2). For a 48 nm thick tungsten film, only nanograins are observed (fig.2a). At the

opposite, for a 175 nm thick tungsten films there are only lamellar structures (fig.2c). Figure 2b (94 nm of thickness) presents an intermediate surface morphology between these two textures. Indeed, the lamellar structure is predominant and some nanograins are still present.

A mass production of layer, using a pure tungsten target with the same growth parameters, has been performed. Same results are obtained with a good reproductibility of the observed phase (XRD results), related to the surface microstructure (AFM studies).

3.3. Influence of the target cleaning

To observe the influence of the target cleaning before the tungsten deposition, two films have been grown, with the same thickness (86 nm determinate by XRR). Only target cleaning time changes : 10 min and 60 min.

XRD analysis results are presented in figure 3. The oxidized tungsten W_3O is the major phase when the target cleaning is 10 minutes (fig.3a). This last phase disappears totally when the target cleaning time is more important (60 min). In fig.3b no more W_3O peaks are observed and the only one peak present is the (110) W.

Figure 4 a and b shows AFM images of tungsten thin films after target cleaning for 10 and 60 min respectively. Films have the same thickness, 86 nm. Both nanograins and lamellar structures are observed when only a 10 min target cleaning is performed. The lamellar structure is the only one observed with a 60 min of target cleaning.

3.4. Growth of a pure W layer after WO_3 layer deposition phase

The objective of this work is to realize multilayer $[W/WO_3]_n$ with pure W target in order to study the mechanical properties. Three thin films of tungsten with a fictitious WO_3 layer have been performed with different target cleaning period before W layer deposition: 1 min, 3 min and 5 min.

XRD patterns analysis of these three films have been performed. They are similar. For instance, figure 5 represents tungsten thin film XRD diagrams after 1 min of target cleaning between WO_3 “fictitious” film and W film.

The surface microstructure, and the roughness (0,47 nm) are the same for the three experiments (fig.6). It shows the only presence of lamellar microstructure.

4. Discussion

XRD patterns analysis (fig.1) shows the dominant presence of the oxidized tungsten W_3O peaks with a (002) preferential orientation for all samples thinner than 100 nm and without target cleaning. When the thickness increases, W peak (110) appears until it becomes majority. In fig.1c) the thickness is too thick to see the peak of the W_3O intermediate phase, present in the first step of the tungsten growth. For 175 nm thick films, only the W peaks (110) are observed. This suggests that when the growth is carried on, the W_3O diffraction peak decreases progressively and disappears completely for a layer thickness higher than 175 nm in favour of W (fig.1c). The oxidized tungsten W_3O peaks aren't present for all samples thinner than 100 nm and performed with a target cleaning (fig.3b). These results suggest that the W_3O phase is related to a target pollution between two growth runs. In sputtering, this phenomenon is currently observed [16]. 60 min of target cleaning at 150 Watt are necessary to remove the oxidized layer formed at the target surface between two runs (few hours). This procedure allows to obtain a pure W layer (fig.3b), even if the tungsten layer thickness is smaller than 100 nm. Experimental XRD patterns show the only presence of W peaks. These patterns lead to the determination of the tungsten Wolfram thin film cell parameters (a=b=c=3,179 Å).

Concerning the morphology of the surface of the layer, when only W_3O peaks are observed in XRD patterns, the surface presents the same nanograins morphology (fig.2a). When both W_3O and W peaks are present in XRD patterns a lamellar structure with still some nanograins is observed (fig.2b). When only W peaks are present in XRD patterns, only the lamellar structure is observed (fig.2c). The same evolution of surface microstructure exists when the time of the target cleaning is changed. With 10 min (fig.4a), both nanograins and lamellar structures are observed, as for 100 nm fig.2b). With 60 min, only the lamellar surface structure is observed

(fig.4b), as for 194 nm fig.2c). It's then possible to correlate the surface morphology thin films to the layer phase composition : W_3O phase presents a nanograin microstructure whereas pure W phase has a lamellar structure. These results are confirmed by the AFM surface analysis performed on the sample grown with the target cleaning. We observed in fig. 4b the lamellar morphology correlated to the pure tungsten Wolfram XRD patterns.

The objective of our work is to study the mechanical properties of nanolaminated $[W/WO_3]_n$ multilayers. The structure consists to a periodic stacking of two layers : W Wolfram and WO_3. WO_3 layers are deposited by a reactive RF-puttering. Then, the target surface is probably oxidized during the WO_3 layer deposition. Nevertheless, during this deposition, the target surface oxidation is much lower than between two runs. Indeed it is continually sputtered and then cleaned by Ar^+ ions. The principal W_3O peak (002) at 35,3° is not observed (fig.5) even with 1 min of target cleaning performed before the W layer growth. Only W (110) peak is represented in the XRD pattern, which indicate that the tungsten layer is constituted of pure W Wolfram. Then 1 min of target cleaning before the W Wolfram layer growth is enough to remove the oxidized layer to the target surface. This result is compatible with the elaboration of nanolaminated structure.

5. Conclusion and future outlook

W_3O phase is observed in tungsten thin films with thicknesses smaller than 100 nm and performed without target cleaning. When the thickness increases, the W_3O phase decreases progressively to disappear completely for a layer thickness higher than 175 nm, in consideration of W Wolfram. When a 60 min target cleaning is performed, only W Wolfram is present. In this paper we correlated the morphology surface with the stoechiometry layer : W possess a lamellar structure; W_3O a nanograins structure.

Moreover we demonstrate that it's possible to realize multilayer $[W/WO_3]_n$ without the presence of W_3O phase in W films by a 1 min target cleaning performed after WO_3 reactive sputtering deposition and before the W layer growth.

References

[1] S. Vepreck, S. Reiprich, Thin Solid Films 268 (1995) 64-71

[2] K.K. Shih, D.B. Dove, Appl. Phys. Lett. 61 (6) (1992) 654-656

[3] R. Cammarata, Thin Solid Films 240 (1994) 82-87

[4] P. Goudeau, K. Badawi, A. Naudon, N. Durand, Mat. Res. Soc. Symp. Proc. 308 (1993) 713-718

[5] M. Mattsson, Phys. Rev. B, Condens. Matter. 58 (16) (1998) 11015-11022

[6] E. Maseti, M. Grilli, G. Dautzenberg, G. Macrelli, M. Adamik, Sol. Energy Mater. Sol. Cells. 56 (3-4) (1999) 259-269

[7] C. Lo, H. Wang, P. Gilman, Mat. Res. Soc. Symp. Proc., 505 (1998) 427-432

[8] Handbook of chemistry and physics, 73RD, edition 1992-1993

[9] M. Arita, I. Nishida, Jpn. J. Appl. Phys. 32 (1993) 1759-1764

[10] Y. Shen, Y. Mai, J. Mat. Sci. 36 (2001) 93-98

[11] A. Katagiri, M. Suzuki, Z. Takechara, J. Electrochem. Soc. 138 (3) (1991) 767-773

[12] W.R. Morcom, W.L. Worrell, H.G. Sell, I. Kaplan, Metallurgical Transactions 5 (1974) 155-161

[13] G. Hagg, N. Schonberg, Acta Cryst. 7 (1954) 351-352

[14] Y. Shen, Y. Mai, Mat. Sc. Engineering A284 (2000) 176-183

[15] I.A. Weerasekera, S. Ismat Shah, D. V. Baxter, K. M. Unruh, Appl. Phys. Lett. 64 (24) (1994) 3231-3233

[16] C. Sant, M. Ben Daia, P. Aubert, S. Labdi, P. Houdy, Surf. Coat. Technol. 127 (2000) 167-173

Reference number of manuscript : J/PI.31

List of Graphics Captions

Fig. 1. XRD patterns of tungsten thin films with different thicknesses a) 48 nm , b) 94 nm and c) 175 nm.

Fig. 2. AFM morphology of tungsten films with different thicknesses a) 48 nm, b) 94 nm and c) 175 nm.

Fig. 3. XRD patterns of tungsten thin films (86 nm) after a target cleaning of a) 10 min and b) 60 min before deposition.

Fig. 4. AFM images of tungsten thin films (86 nm) after a target cleaning of a) 10 min and b) 60 min before deposition.

Fig. 5. XRD pattern of tungsten thin film (50 nm) after 1 min of target cleaning performed between WO_3 “fictitious” film and W film.

Fig. 6. AFM images of tungsten thin film (50nm) after 1 min of target cleaning performed between WO_3 “fictitious” film and W film.

Reference number of manuscript : J/PI.31

Fig. 1.

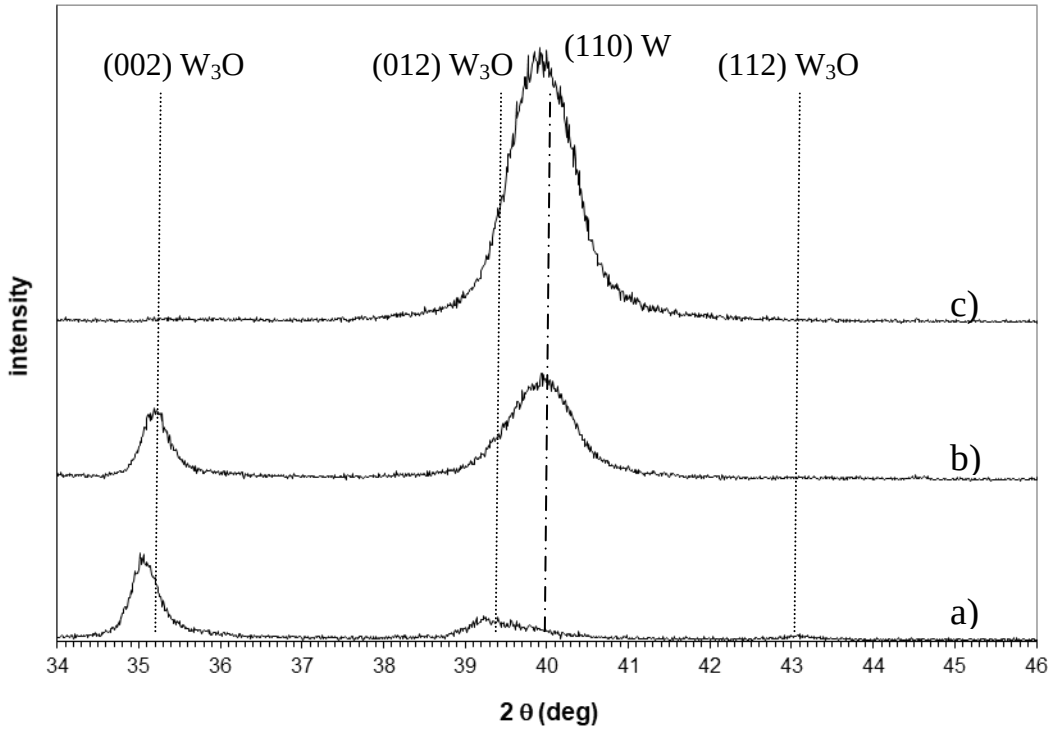

Reference number of manuscript : J/PI.31

Fig. 2.

a)

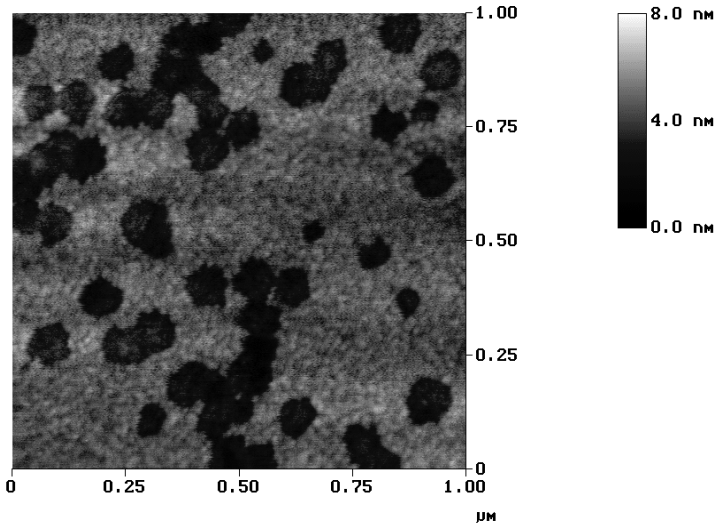

b)

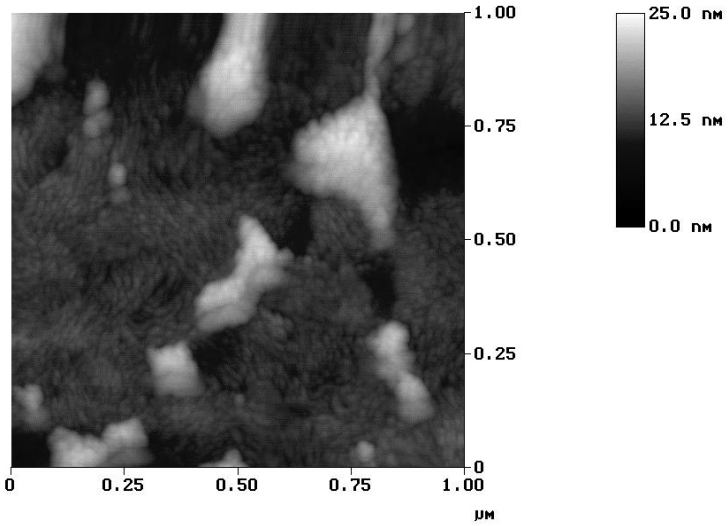

c)

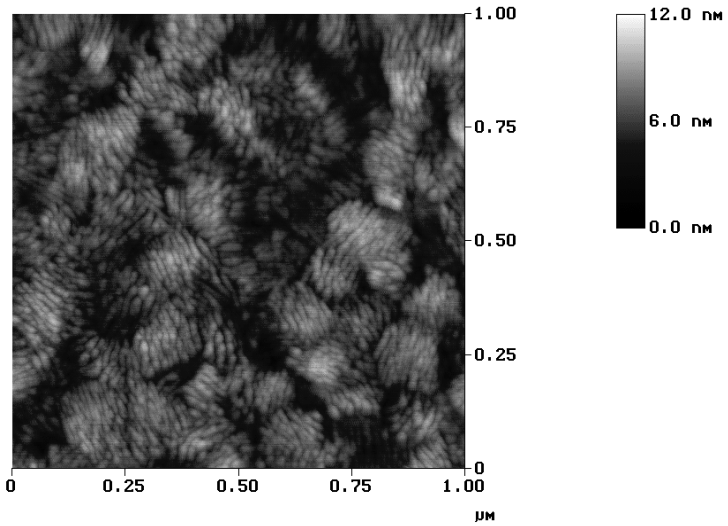

Reference number of manuscript : J/PI.31

Fig. 3.

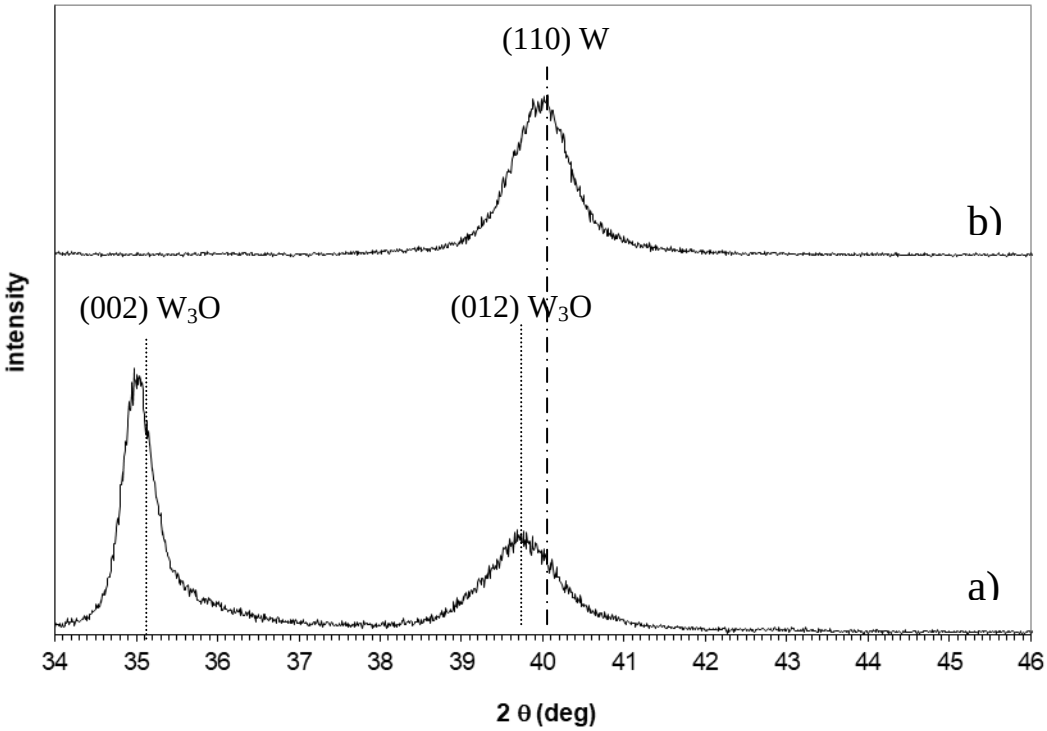

Reference number of manuscript : J/PI.31

Fig. 5.

a)

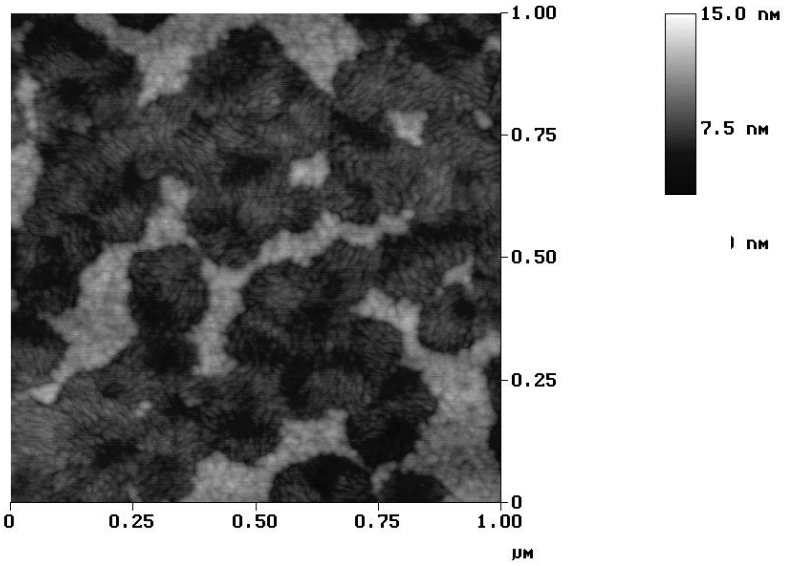

b)

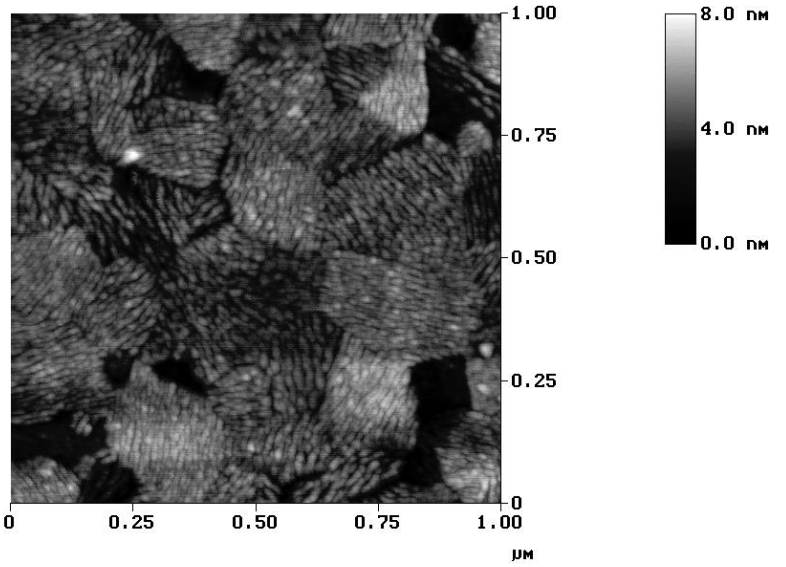

Reference number of manuscript : J/PI.31

Fig. 6.

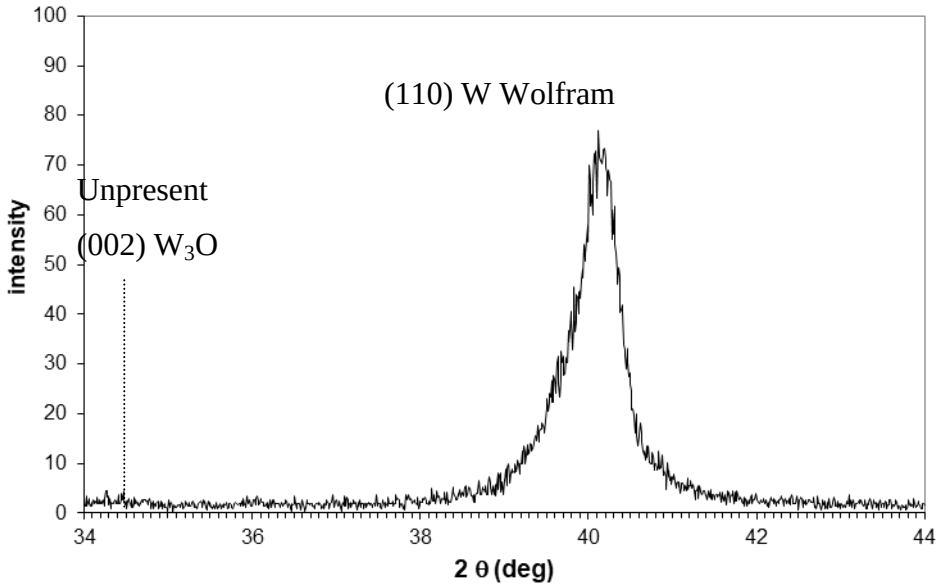

Reference number of manuscript : J/PI.31
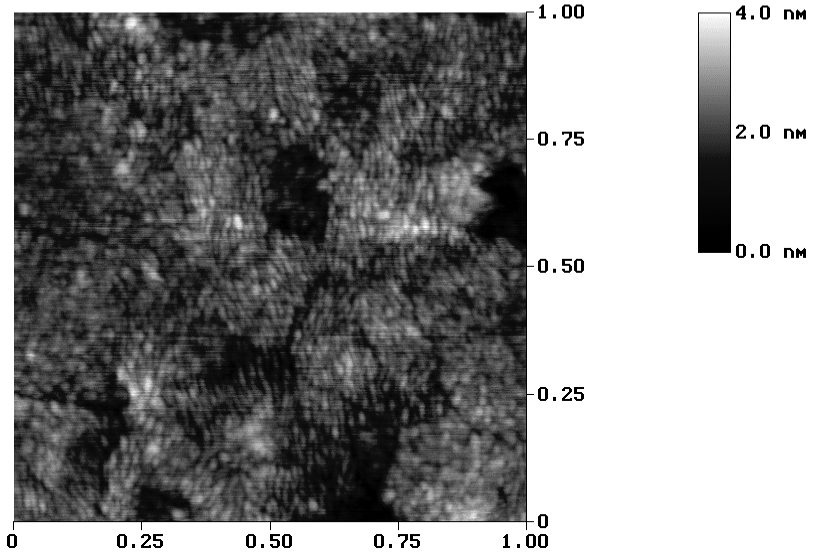
Fig 7.